Polymer Chemistry

COMMUNICATION

Cite this: *Polym. Chem.*, 2017, **8**, 370

Received 8th November 2016,
Accepted 24th November 2016

DOI: 10.1039/c6py01956k

www.rsc.org/polymers

One-pot synthesis of inorganic nanoparticle vesicles *via* surface-initiated polymerization-induced self-assembly†

Yang Zheng, Yucheng Huang, Zaid M. Abbas and Brian C. Benicewicz*

The first case of surface-initiated polymerization-induced self-assembly (SI-PISA) of inorganic nanoparticles (NPs) into single-walled vesicles is reported. A solvent-miscible brush was first grafted onto 15 nm silica NPs, and self-assembly was subsequently induced by the polymerization of a second brush that was solvent-immiscible. Self-assembly occurred *in situ* with the SI-polymerization of the second brush. This approach establishes a method to prepare nanovesicles at relatively high NP concentration, and does not require any post-polymerization processing. Moreover, this strategy provided an opportunity to observe the evolution of nanovesicle formation from well-dispersed NPs, that aided our understanding of how surface-grafted polymers direct the vesicular assembly of NPs.

Self-assembly of inorganic nanoparticles (NPs) into hierarchical architectures is a promising approach toward novel functional materials.[1–3] Of all the self-assembled structures (strings, tubes, spheres, vesicles, *etc.*), nanovesicles are of particular interest because of their hollow structures that enable applications in drug delivery,[4] catalysis,[5] bioimaging,[6] and cancer therapy.[7,8] In recent literature, such vesicles were prepared by coating inorganic NPs with amphiphilic ligands[9] or polymers.[10,11] As for polymer-directed self-assembly, both mixed brush grafted NPs[4,10] and block copolymer tethered NPs[5,7,11] have been prepared that successfully assembled into thin-layer vesicles. Typically, the polymer-grafted NPs were first prepared in a good solvent for each component followed by purification steps to remove free polymers. Then, self-assembly was triggered by addition of a selective solvent[7,9] or film rehydration,[10,11] which required multiple steps of sample preparation and was limited by low NP concentration. For example, NP concentration was kept below 260 μg ml^{-1} for the film rehydration method;[3,8] Nie *et al.* studied the concentration effect on self-assembly of PEG-*b*-PCL tethered gold NPs by solvent switching and found that nanoscale vesicle formation was limited to particle concentrations less than 250 μg ml^{-1}, otherwise huge submicron-sized assemblies were formed.[12] Thus, gram-scale production of such hybrid vesicular assemblies still remains a challenging task.

Recently, polymerization-induced self-assembly (PISA) emerged as a facile self-assembly method toward stable nano-objects with a variety of morphologies including spheres, worms and vesicles.[13] Compared with the traditional method of preparing block copolymer assemblies, PISA has the advantages of a one-step reaction and relatively high solid content (20–50% w/w).[14] The self-assembly mechanism relies on the chain-extension of a solvent miscible macro-initiator with a solvent-immiscible polymer. Self-assembly occurred during polymerization when the immiscible block reached a critical length. However, to our knowledge, this method has been rarely applied to direct the self-assembly of inorganic nanoparticles. We recently reported the first case of surface-initiated polymerization-induced self-assembly (SI-PISA) by polymerizing benzyl methacrylate from SiO_2-*g*-(PHEMA, CPDB) NPs that resulted in ordered 1D nano-strings.[15] However, we did not observe higher ordered assemblies before macroscopic phase separation occurred, probably due to the poor stabilizing effect of PHEMA in methanol.[16]

Herein we describe an improved design of surface-initiated polymerization-induced self-assembly (SI-PISA) that leads to stable 3D assemblies at high NP concentration (~10 mg ml^{-1}). Self-assembly occurred spontaneously during polymerization, which is analogous to PISA of block copolymers. However, in contrast to block copolymer PISA, the polymer chains were anchored onto inorganic NP surfaces, forming mixed brush grafted NPs which directed the self-assembly of NPs into hybrid assemblies. In the current approach homopolymer brushes were first grafted onto inorganic NPs that were compatible with the target solvent (ethanol) to disperse NPs, and then a second population of brushes was polymerized that were immiscible in the solvent. As the growth of the second brush population proceeded, the increased "solvophobicity" of the immiscible chains induced interparticle collapse, and

Department of Chemistry and Biochemistry, University of South Carolina, Columbia, SC, 29208, USA. E-mail: Benice.sc.edu

†Electronic supplementary information (ESI) available. See DOI: 10.1039/C6PY01956K

This journal is © The Royal Society of Chemistry 2017

directed the self-assembly of inorganic cores. Hybrid vesicles with sizes on the nanometer scale were produced *in situ* with polymerization, without the need for any post-polymerization steps. Moreover, by taking samples periodically after the polymerization started, we observed the entire evolution process from well-dispersed NPs to short nanostrings, to nanorings, to nanovesicles and eventually, micron-sized aggregates, that provided interesting mechanistic insights about the birth and death of NP vesicles.

The mixed brush grafted NPs were synthesized using a sequential surface-initiated RAFT polymerization strategy that provided precise control over the composition of both brushes. In the first step, SiO_2-*g*-(PHPMA, CPDB) NPs were prepared as shown in Scheme 1(A). Poly(hydroxypropyl methacrylate) (PHPMA), which has been used to successfully stabilize 3D assemblies of block copolymer PISA was grafted onto 15 nm silica NPs using surface-initiated RAFT polymerization in DMF at 65 °C. PHPMA with a molecular weight of 16 kDa and 0.1 ch per nm^2 graft density was achieved, which was confirmed by NMR and TGA characterization (Fig. S1†). Chain-end RAFT groups were removed by reacting with excess AIBN, to deactivate the first polymer brush.[17,18]

Then, a second RAFT agent was attached onto the unreacted surface with 0.1 ch per nm^2 graft density, which was calculated from the characteristic UV absorption at 304 nm and TGA data (see ESI† for details). The resulting NPs, SiO_2-*g*-(PHPMA, CPDB) appeared as viscous pink solids after solvent removal, and could be easily re-dispersed in ethanol and used as precursors to vesicular assemblies.

Surface-initiated polymerization of a second monomer benzyl methacrylate (BzMA) from SiO_2-*g*-(PHPMA, CPDB) was conducted at 70 °C with the molar ratio of RAFT : BzMA : ACVA = 1 : 1000 : 0.15. Ethanol was added as solvent to achieve ~10 mg ml^{-1} NP concentration. Both reaction solvent and monomer were carefully selected as ethanol is a good solvent for PHPMA grafted NPs and BzMA monomer, but a poor solvent for PBzMA. As the polymerization proceeded, the growing PBzMA chains promoted self-assembly by interparticle collapse, while PHPMA chains served as stabilizers to prevent uncontrolled agglomeration (Scheme 1B).

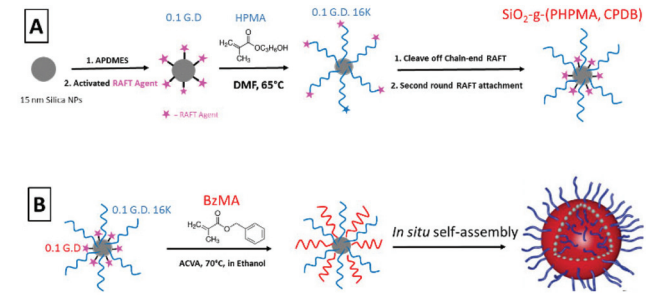

Scheme 1 (A) Synthesis of SiO_2-*g*-(PHPMA, CPDB). (B) One-pot surface-initiated RAFT polymerization-induced self-assembly of grafted NPs into vesicles.

The formation of assemblies during polymerization could be observed from the turbidity changes of the reaction solution. A small sample was withdrawn from the reaction flask periodically throughout polymerization and the visual appearance of each sample is shown in Fig. 1A. The polymerization

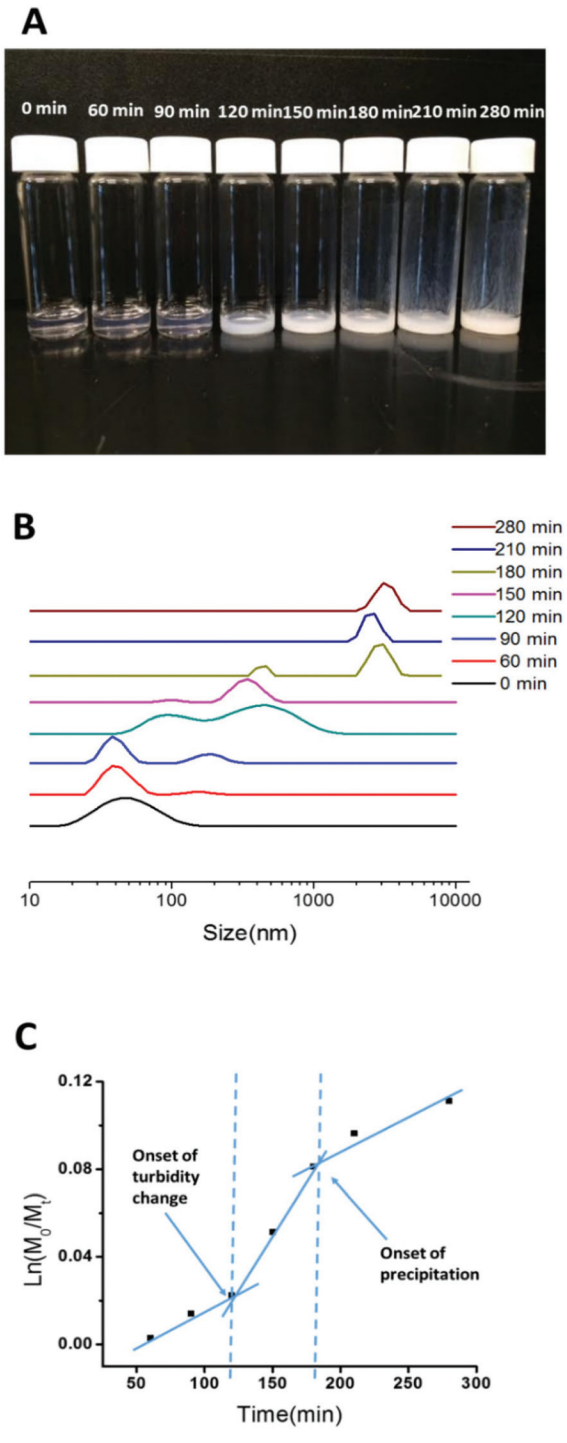

Fig. 1 (A) Visual appearance of each sample withdrawn during polymerization. (B) DLS of each sample withdrawn during polymerization. (C) Polymerization kinetics of surface-initiated RAFT polymerization of BzMA from SiO_2-*g*-(PHPMA, CPDB) in ethanol at 70 °C.

system started as a clear, light-pink, homogenous solution, which remained unchanged during the first 1.5 hours. The onset of turbidity changes occurred at 120 min, when a slightly turbid solution was observed. At this time, the solution was still homogenous with no macroscopic precipitate. The turbidity increased with time and macroscopic precipitates were observed after 180 min. White precipitates formed and adhered onto the wall of glass vials (Fig. 1, right 3 vials in C), indicating formation of unstable assemblies.

To better understand the self-assembly mechanism, each sample displayed in Fig. 1A was analysed by dynamic light scattering (DLS) to obtain NP size distributions (Fig. 1B). The trend in nanoparticle diameter measured by DLS agreed with visual observations, and clearly indicated the formation of assemblies. At 0 min, only one peak at 45 nm was observed, which corresponded to individually dispersed SiO_2-*g*-(PHPMA, CPDB) NPs. A second peak centered at *ca*. 200 nm appeared soon after the reaction started, indicating initial formation of aggregates. As the polymerization proceeded, the individual NP peak gradually disappeared, while the aggregates peak increased as well as shifted towards larger size. As the polymerization proceeded even further, a new peak at micron-scale size appeared, and quickly became the dominant size in the distribution. These data indicated that there were two stages of self-assembly where well-dispersed nanoparticles first self-assembled into nanoscale assemblies, which then further evolved into microscale assemblies.

The polymerization of BzMA was also monitored by ^{1}H NMR to obtain monomer conversion. Interestingly, the polymerization kinetics curve, $\ln(M_0/M_t)$ *vs.* time, displayed three different stages (Fig. 1C), even though the reaction temperature remained constant at 70 °C. Additionally, the three stages were separated by specific points correlated with the onset of initial cloudiness and the onset of precipitate formation, which provides some interesting mechanistic insights. The kinetics of the first stage at 0 to 120 min corresponded to normal solution based surface-initiated controlled radical polymerization, when short PBzMA chains grew from well-dispersed NPs. The rate of polymerization increased in the second stage from 120 to 180 min, which corresponded to the onset of aggregation as observed both visually and by DLS. At this stage, PBzMA chains reached a critical length and nascent assemblies formed with insoluble PBzMA chains collapsing with each other, and the unreacted BzMA monomers preferentially remaining within the PBzMA regime, thus increasing the local monomer concentration. Similar behaviour has been reported in block copolymer PISA in both alcoholic medium and aqueous solution.[19] The third stage, from 180 to 280 min, was marked by the onset of precipitation. At this stage, micron-sized assemblies were formed that tended to precipitate from the reaction medium. As a result, chain-transfer agents and monomers were no longer in the same phase, chain end mobility was restricted, and the reaction kinetics decreased. Overall the M_n of the BzMA chains showed a linear increase with conversion during the entire polymerization period and polydispersity of PBzMA remained below 1.1 (Fig. S3†). The corresponding GPC traces of PBzMA chains shifted to higher molecular weights during the polymerization, with unimodal distributions, (Fig. S4†) indicating that the polymerization of BzMA proceeded with good control, and resulted in a well-defined mixed brush polymer structure. The details of the reaction time, monomer conversions, GPC data, DLS data, and visual appearance obtained for a series of SiO_2-*g*-(PHPMA, PBzMA) NPs are summarized in Table S1.†

The morphologies of the self-assembled structures during polymerization were investigated by transmission electron microscopy (TEM) and revealed the early formation and growth of nano-sized assemblies into thin-layer vesicles. Initially, PHPMA grafted NPs were well-dispersed in ethanol (0 min, Fig. 2A). When the polymerization was initiated, NPs first organized into short strings of a small number of NPs (60 min Fig. 2B). With continued growth of the PBzMA, the connectivity of the short strings increased and formed ring-like structures which then served as templates for fully enclosed vesicles (Fig. 2C and D, 90 min). Samples at 120 min contained highly mixed morphologies of nascent vesicles, half-vesicles, disks and dispersed NPs (Fig. 2E and F), which was consistent with DLS data that showed a fairly large polydispersity of sizes. The filling and wrapping of the nanorings into vesicles progressed with time and was mostly complete at 150 min (Fig. 2G), when most of the observed structures were complete vesicles. DLS data also showed that most components in solution at this time were self-assembled structures with ~340 nm diameter. The duration of the pure vesicle phase was fairly short, probably due to the increased polymerization rate at this stage. By 180 min, most of the vesicle structures had disappeared and were replaced by collapsed structures. Fig. 2H show the progression involving wall thickening, followed by intervesicle collapse. Eventually (280 min Fig. 2I), all the vesicles had evolved into micron-sized clusters with irregular shapes.

The hollow nature of self-assembled structures at 150 min after reaction started was further revealed by both TEM and scanning electron microscopy (SEM) studies. Fig. 3A shows a close-up view of one vesicle structure with a broken fraction of its shell. The peripheral region has the darkest contrast, representing a thin layer of vesicle walls collapsed on a flat TEM grid. The left part of inner region represents the double layer of NPs which is a typical projection of a 3D thin-layer hollow sphere onto a 2D image. The right-hand section of the inner space showed the lightest contrast and was apparently composed of a single-layer of 15 nm NPs, which is the result of a partially enclosed shell. SEM images (Fig. 3B) further confirmed that the vesicles have hollow cavities enclosed by a walls made from the grafted nanoparticles.

Based on the step-by-step assembly process from dispersed NPs to nanovesicles presented in Fig. 2, we propose a detailed mechanism for the formation of vesicles from the SI-PISA of NPs (Scheme 2). When the insoluble PBzMA chains reached a critical length, the mixed brush grafted NPs underwent a localized phase separation of the soluble PHPMA chains from the insoluble PBzMA chains. Initial self-assembly occurred by

 This journal is © The Royal Society of Chemistry 2017

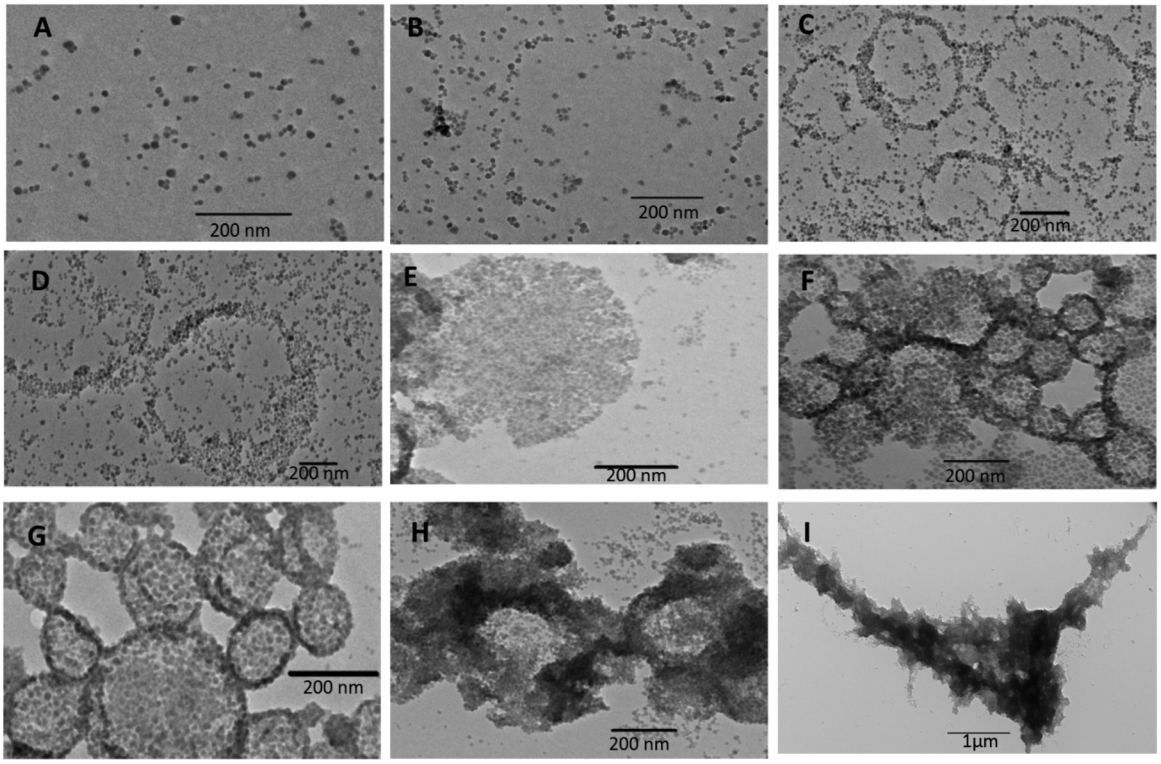

Fig. 2 Representative TEM images of the assemblies at different polymerization times: 0 min (A), 60 min (B), 90 min (C, D), 120 min (E, F), 150 min (G), 180 min (H), 280 min (I).

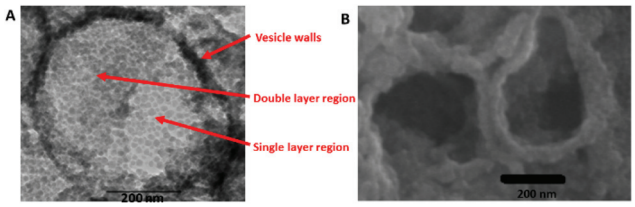

Fig. 3 (A) Close-up TEM view of an individual self-assembled vesicle with broken shell (left image). (B) SEM image of self-assembled vesicles showing inner cavities and single-layer walls (right image).

interparticle collapse between PBzMA domains, forming short strings and nanorings. The nanorings directed the orientation and addition of further NPs to grow inward, forming nanodisks composed of NPs embedded in the collapsed PBzMA domain that were stabilized by PHPMA chains extending into the solvent. The round-shaped disks then formed wedge shaped defects around their perimeter, which facilitated folding of the nanoparticle disks into single-walled vesicles.

In order to demonstrate SI-PISA as a general one-step strategy towards well-defined nanovesicles, we further explored another system using SiO_2-*g*-(PMAA, PBzMA) NPs as building blocks. The synthetic route is same as the SiO_2-*g*-(PHPMA, PBzMA) case described above, but poly(methacrylic acid) (PMAA) (23 kDa) was used as stabilizing brush instead of PHPMA (Scheme S2†). As a result, similar self-assembly behaviour was observed from surface-initiated polymerization of

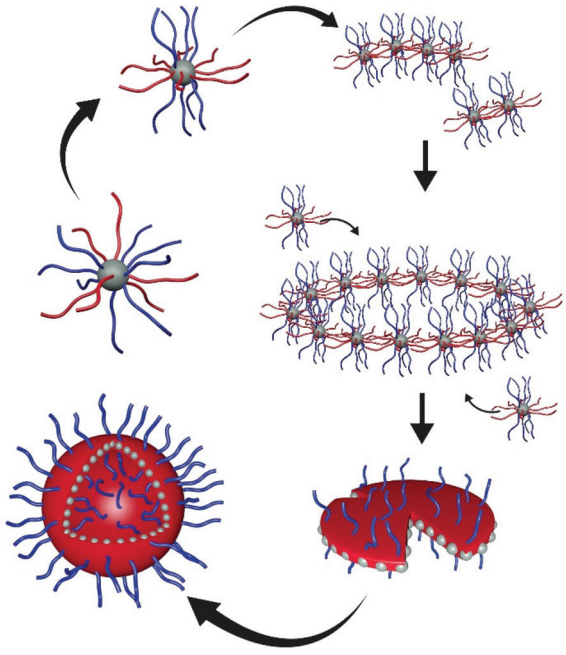

Scheme 2 Proposed mechanism of surface-initiated polymerization-induced self-assembly of NPs into nanovesicles.

BzMA using SiO_2-*g*-(PMAA, CPDB) as stabilizer. Vesicles were formed during polymerization at 10 mg ml^{-1}. Additionally, we also observed the intermediate stages as rings, disks, half

enclosed vesicles, and fully enclosed vesicles (Fig. S5†). It is also worth mentioning that an early attempt to perform SI-PISA using shorter PMAA (5.8 K) as stabilizing brushes failed to result in any well-organized structures. Instead, NP clusters in random shapes were observed (Fig. S6†). These observations indicated that the length of the stabilizing brushes plays an important role in the self-assembly process. Understanding the critical molecular length of the stabilizing block would be an interesting topic to further define this SI-PISA strategy.

Conclusions

In conclusion, we demonstrated a facile and efficient way using surface-initiated polymerization to induce self-assembly of inorganic NPs into single-layer nanovesicles. This SI-PISA strategy represents a new aspect of PISA, that utilizes the growth of polymer chains from NP surfaces to direct the self-assembly of inorganic nanoparticles. Compared with the traditional way of preparing hybrid nanovesicles by solvent switching and film rehydration, this newly developed self-assembly method requires no post-polymerization process and can be operated at high NP concentration ($\sim$10 mg ml^{-1}), which is important for large production of such hybrid assemblies. This approach also offered insights into the evolution of nanovesicles, including their birth from well-dispersed NPs and nanorings, and their death into micron-sized aggregates. We believe that this strategy could be further extended to prepare nanovesicles in other media (*i.e.* non-polar solvents and water) with different polymer brush selection. Moreover, we could expect the self-assembly of NPs with various shapes like nanotubes and solid spheres, by fine-tuning the chain length and graft density of the first brush and the graft density of the second brush. We believe that the SI-PISA strategy described in this communication could open up many possibilities of preparing functional hybrid materials from polymer-grafted NPs.

Notes and references

1 M. Grzelczak, J. Vermant, E. M. Furst and L. M. Liz-Marzán, *ACS Nano*, 2010, **4**, 3591–3605.
2 Z. Nie, A. Petukhova and E. Kumacheva, *Nat. Nanotechnol.*, 2010, **5**, 15–25.
3 M. G. Moffitt, *J. Phys. Chem. Lett.*, 2013, **4**, 3654–3666.
4 J. Song, Z. Fang, C. Wang, J. Zhou, B. Duan, L. Pu and H. Duan, *Nanoscale*, 2013, **5**, 5816–5824.
5 T. Bian, L. Shang, H. Yu, M. T. Perez, L.-Z. Wu, C.-H. Tung, Z. Nie, Z. Tang and T. Zhang, *Adv. Mater.*, 2014, **26**, 5613–5618.
6 J. Lin, S. Wang, P. Huang, Z. Wang, S. Chen, G. Niu, W. Li, J. He, D. Cui, G. Lu, X. Chen and Z. Nie, *ACS Nano*, 2013, **7**, 5320–5329.
7 J. He, X. Huang, Y.-C. Li, Y. Liu, T. Babu, M. A. Aronova, S. Wang, Z. Lu, X. Chen and Z. Nie, *J. Am. Chem. Soc.*, 2013, **135**, 7974–7984.
8 K. Niikura, N. Iyo, Y. Matsuo, H. Mitomo and K. Ijiro, *ACS Appl. Mater. Interfaces*, 2013, **5**, 3900–3907.
9 K. Niikura, N. Iyo, T. Higuchi, T. Nishio, H. Jinnai, N. Fujitani and K. Ijiro, *J. Am. Chem. Soc.*, 2012, **134**, 7632–7635.
10 J. Song, L. Cheng, A. Liu, J. Yin, M. Kuang and H. Duan, *J. Am. Chem. Soc.*, 2011, **133**, 10760–10763.
11 J. He, Y. Liu, T. Babu, Z. Wei and Z. Nie, *J. Am. Chem. Soc.*, 2012, **134**, 11342–11345.
12 P. Huang, J. Lin, W. Li, P. Rong, Z. Wang, S. Wang, X. Wang, X. Sun, M. Aronova, G. Niu, R. D. Leapman, Z. Nie and X. Chen, *Angew. Chem., Int. Ed.*, 2013, **52**, 13958–13964.
13 S. L. Canning, G. N. Smith and S. P. Armes, *Macromolecules*, 2016, **49**, 1985–2001.
14 N. J. Warren and S. P. Armes, *J. Am. Chem. Soc.*, 2014, **136**, 10174–10185.
15 Y. Zheng, Y. Huang, Z. M. Abbas and B. C. Benicewicz, *Polym. Chem.*, 2016, **7**, 5347–5350.
16 D. Zehm, L. P. D. Ratcliffe and S. P. Armes, *Macromolecules*, 2013, **46**, 128–139.
17 A. Rungta, B. Natarajan, T. Neely, D. Dukes, L. S. Schadler and B. C. Benicewicz, *Macromolecules*, 2012, **45**, 9303–9311.
18 L. Wang, M. Cole, J. Li, Y. Zheng, Y. P. Chen, K. P. Miller, A. W. Decho and B. C. Benicewicz, *Polym. Chem.*, 2015, **6**, 248–255.
19 A. Blanazs, J. Madsen, G. Battaglia, A. J. Ryan and S. P. Armes, *J. Am. Chem. Soc.*, 2011, **133**, 16581–16587.

This journal is © The Royal Society of Chemistry 2017